



# Enhancement of the surface free energy of PDMS for reversible and leakage-free bonding of PDMS–PS microfluidic cell-culture systems

Ki-Young Song<sup>1,2</sup> · Hongbo Zhang<sup>4</sup> · Wen-Jun Zhang<sup>3</sup> · Ana Teixeira<sup>1</sup>

Received: 27 March 2018 / Accepted: 23 October 2018 / Published online: 9 November 2018  
© Springer-Verlag GmbH Germany, part of Springer Nature 2018

## Abstract

Polydimethylsiloxane (PDMS) has become one of the most widely used materials in the fabrication of microfluidic systems bonded onto glass substrates, especially for cell biology applications. However, PDMS is often unsuitable for building microfluidic systems onto polystyrene (PS) which is the preferred substrate in most cell-culture protocols. In particular, PS is required for culturing many stem cell and primary cell types. Here, we propose a novel approach to building PDMS–PS microfluidic cell-culture systems, specifically realizing a strong and reversible bonding of PDMS on PS without using chemical agents which can have negative effects on cell viability. Our strategy to strengthen the bonding of PDMS to PS surfaces is to increase the surface free energy (SFE) by adjusting the mixing ratio of PDMS base to curing agent and by treating the surfaces of PDMS and PS with O<sub>2</sub> plasma and annealing. Our results show that using this method for PDMS–PS bonding, we are able to produce reliable reversible and leakage-free PDMS–PS microfluidic cell-culture systems.

**Keywords** PDMS · Polystyrene · Bonding · Surface free energy · Microfluidic cell-culture systems

## 1 Introduction

For more than half a century, plastic dishes have been commercially available for *in vitro* cell culture. Most dishes are made from polystyrene (PS) due to its excellent optical transparency, easy molding, and simple sterilization. Moreover, several technologies have been used to optimize PS dish performance for culture of various cell lines and primary cells, enhancing cell attachment (Ryan 2008). Today, most cell-culture protocols and guidelines are developed based on PS petri dishes or flasks.

Microsystems have received great attention in cell biology after biocompatible and flexible polymeric organosilicon compounds were introduced. In particular, polydimethylsiloxane (PDMS) has many applications in microsystems due to its remarkable physical and chemical properties, such as wide temperature range (– 100 to 200 °C), low stiffness (~ 1 MPa), chemical inertness, biocompatibility, optical transparency, and low cost (Lowe et al. 2008; Seghir and Arscott 2015), which includes applications such as microfluidic devices (Friend and Yeo 2010; Li et al. 2017), patterned cell-culture systems (Tanaka et al. 2014; Wang et al. 2013), and DNA and protein microanalysis systems (Kovarik et al. 2012, 2013). For applications that involve cells cultured on microfluidics systems, combined PDMS-based microfluidic systems on PS substrates are advantageous as PS is the substrate of choice for established standard cell-culture protocols (Halldorsson et al. 2015). Importantly, analysis of cells cultured on microsystems is often facilitated by separating the PDMS chips from the substrate, which relies on reversible bonding between PDMS and PS.

Standard soft lithography and replica molding processes are commonly applied to fabricate PDMS chips (Qin et al. 2010; Xia and Whitesides 1998). Conventionally, the PDMS chips are bonded onto substrates irreversibly by

✉ Ki-Young Song  
kiyoungsong@bit.edu.cn

<sup>1</sup> Department of Medical Biochemistry and Biophysics, Karolinska Institutet, Stockholm, Sweden

<sup>2</sup> School of Mechatronic Engineering, Beijing Institute of Technology, Beijing, China

<sup>3</sup> Department of Mechanical Engineering, University of Saskatchewan, Saskatoon, SK, Canada

<sup>4</sup> School of Mechanical and Power Engineering, East China University of Science and Technology, Shanghai, China

various bonding approaches: (1) oxidation bonding: surface oxidation by oxygen plasma (Duffy et al. 1998) or corona discharge (Haubert et al. 2006) introduces silanol (Si–OH) groups on the surface of PDMS to produce a surface with hydrophilic properties as well as to increase its surface free energy (SFE). This surface modification results in an irreversible bonding, through siloxane covalent bonds (Si–O–Si), with silicon-based substrates, providing a simple and stable bonding procedure. After the oxidation pretreatment, however, the bonding step must be completed within minutes to avoid surface rearrangements which lower the SFE and thereby increase the hydrophobicity of the surface (Lee et al. 2003). Furthermore, oxidation bonding is not applicable to non-silicon-based materials, such as thermoplastics. (2) Adhesive bonding: a thin partially cured PDMS film acts as a glue between a substrate and a PDMS chip. The unreacted silicon hydrides in the glue are made to react by an additional curing (baking) process to provide uniform properties of PDMS in micro-structures (Abdelgawad et al. 2008; Wheeler et al. 2004). However, this bonding approach requires an accurate time control to obtain partially cured PDMS at low temperatures, making the process time-consuming. Furthermore, the adhesive bonding approach often leads to clogging problems due to the glue, which limits the applicable sizes of micro-structures in PDMS chips (Shiroma et al. 2016). (3) Chemical modification bonding: the surfaces of the PDMS chip as well as of the substrate are chemically modified to adhere at the interface. The chemical bonding approach is typically applied to bond non-silicon-based thermoplastic substrates, including PS, to silicon-based PDMS by amine–PDMS, silane–PDMS, or amine–epoxy bond formation at the interfaces (Im et al. 2009; Lee and Chung 2009; Sunkara et al. 2011; Tang and Lee 2010). (4) Other approaches such as sandwich bonding (Shiroma et al. 2016) and lamination bonding (Xie et al. 2017).

The bonding approaches mentioned above are not appropriate for achieving tight adhesion of PDMS chips on PS surfaces. The oxidation and adhesive bonding approaches are not applicable to PS dishes, since a PS dish is neither silicon-based nor heat-resistant at the high temperatures that are required to shorten the curing times of PDMS. A PS dish starts to deform at around  $\sim 80$  °C. Permanent (irreversible) bonding of PDMS onto PS surfaces can be achieved by chemical surface modification of the PS surface with a silane reagent, (3-aminopropyl) triethoxysilane (APTES), forming a covalent bond with PS. The PS surface is first treated with oxygen plasma, and then coated with an aqueous solution of 1% APTES (v/v) for 20 min. An oxygen plasma-treated PDMS device attaches firmly to the top of the treated dry PS surface within a few minutes at room temperature (Sonney et al. 2015; Sunkara et al. 2011). Although this chemical surface

modification approach is effective, the process includes several time-consuming steps. More importantly, APTES is a potentially hazardous chemical, which can cause loss of viability of sensitive cells, such as primary and stem cells.

As discussed above, various PDMS–PS systems are available with irreversible (or high strength) bonding; however, irreversible bonding often does not meet the requirements of PDMS–PS cell-culture systems. Several reversible PDMS bonding methods are available, such as adhesives (Vézy et al. 2011), magnetism (Igata et al. 2002), vacuum (Le Berre et al. 2006), and biomimetic structure (Wasay and Sameoto 2015). However, these methods require complex fabrication processes and are not cost effective.

In this study, we developed a novel and simple approach for reversible and leakage-free PDMS–PS bonding to build PDMS–PS microfluidic cell-culture systems. This approach can increase the SFE of PDMS and strengthen the adhesion of PDMS on PS without chemical agents. We investigated whether the adhesion of PDMS to PS could be regulated by the stiffness of PDMS. The stiffness of PDMS can be tuned by adjusting the concentration of curing agent ( $R$ ), the curing temperature, and the curing time (Seghir and Arscott 2015). The concentration of the curing agent has been shown to control PDMS stiffness (Ochsner et al. 2007; Palchesko et al. 2012; Teixeira et al. 2009; Wang et al. 2014). Furthermore, the curing temperature and the curing time have been shown to control the stiffness of PDMS (Johnston et al. 2014; Liu et al. 2009; Palchesko et al. 2012; Seghir and Arscott 2015).

PDMS–PS bonding can be improved by increasing the SFE of PDMS and by treating the surface with  $O_2$  plasma. However, the SFE of PDMS treated with  $O_2$  plasma decreases within a few minutes after the treatment (Lamberti et al. 2012). We found that the treatment of PDMS and PS surfaces with  $O_2$  plasma (for 1 min) increased the SFEs of both the surfaces, reinforcing the adhesion between the surfaces. An additional annealing process (at 65 °C for 1 h) of both the PDMS and PS surfaces enhanced the adhesion and allowed stabilization of the higher SFE for a longer period of time ( $> 3$  days). Our approach was verified by contact angle (CA) and Young's modulus measurements on PDMS and by measurements of the adhesion force between PDMS and PS. In brief, our data revealed that the ratio of PDMS base and curing agents in the range of 11–13 followed by surface treatment with  $O_2$  plasma and annealing can provide an appropriate reversible PDMS–PS bonding with tight sealing. The reversible and leakage-free PDMS–PS bonding allows PDMS chips to be separated easily and completely from PS surface with a minimal external force ( $< 8$  N). Furthermore, we addressed the toxicity of APTES on primary cell culture, illustrating the advantages of our reversible PDMS–PS bonding.

## 2 Experimental

### 2.1 Materials

PDMS was prepared by mixing the base and curing agent of a commercial silicon elastomer (Sylgard 184, Dow Corning) at weight ratios,  $R_s = \text{PDMS base/curing agent}$ , of 10, 11, 13, 15, 17, and 20. SU-8 2100 (MicroChem) was used to prepare molds for soft lithography. For the adhesion test, standard 60 mm PS culture dishes (TC dish 60, Standard, Sarstedt) were used as purchased. Two food dyes, red and green, were used for leakage test. For cell culture, 50  $\mu\text{g/ml}$  aqueous collagen solution (Rat tail type I; Corning) in 0.02% acetic acid (Sigma-Aldrich) and an aqueous solution of 1% APTES (Sigma-Aldrich) solution (v/v) were used to coat the PS dishes.

### 2.2 Sample preparation and microfluidic device fabrication

We poured the PDMS mixtures in separate PS dishes. The mixtures were degassed in a vacuum chamber for 30 min and cured at 65 °C for 2 h in an oven. The cured PDMS samples were then cut in cylinder shapes with 8 mm in diameter and 5 mm in height using a biopsy puncher (Kai Medical). The test samples were used to measure the contact angle (and calculate the SFE), Young's modulus, and adhesion force of PDMS at various  $R$ . Furthermore, we investigated the effects of  $\text{O}_2$  plasma treatment (for 1 min under  $\sim 320$  mTorr and  $\sim 30$  W RF) and annealing (for 1 h at 65 °C) of PDMS on these properties. In addition, the effects of the surface treatment (i.e.,  $\text{O}_2$  plasma treatment and annealing) of PS on the adhesion to PDMS were investigated.

We prepared microfluidic devices by standard soft lithography and replica molding processes (Qin et al. 2010; Xia and Whitesides 1998) with the PDMS mixtures (additional  $R_s = 30$  and 40) for sagging and leakage tests. The microfluidic device included two parallel microchannels with the dimensions of 1500  $\mu\text{m}$  in width and 100  $\mu\text{m}$  in height apart from each other in 200  $\mu\text{m}$  (Fig. 1a). The dimensions of the design are commonly used for microfluidic cell-culture systems. The PDMS mixtures used for the microfluidic devices were degassed and cured in the same manner as the test samples. After cleaning the cured microfluidic devices by sonication under Ethanol for 5 min and DI water for 5 min consecutively, we prepared the devices with and without the surface treatments to examine the leakage of the devices. All the devices used were cleaned in the same condition before applying the surface treatments.

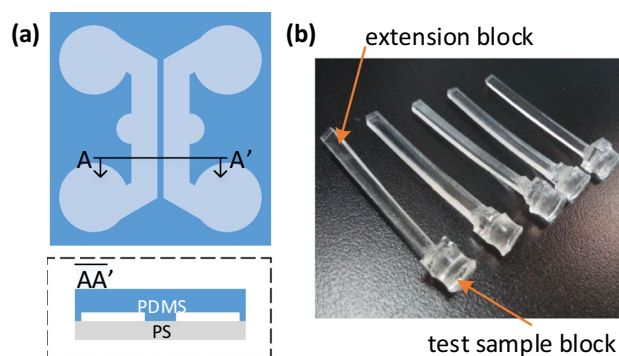


**Fig. 1** Preparation of the experimental setup: **a** schematics of the microchannels (not drawn to scale), and **b** optical image of the test samples with the extension for adhesion test

### 2.3 Measurement of properties of PDMS and adhesion on PS surface

The CA was measured by a contact angle goniometer, JC2000C (Powereach, Shanghai, China) and used to calculate the SFE. The PDMS test sample was placed on the platform of the equipment, and 15  $\mu\text{l}$  pure water drop was laid on top of the test sample to measure the contact angle and the SFE using the image. Five test samples were tested for each condition, i.e.,  $R$  and the surface treatment.

The Young's modulus and the adhesion force of the PDMS test samples were measured by a tensile and compression testing machine, HY-U350 (Shanghai HengYi Precision Instrument Co., Ltd., China). We used the cylindrical test sample to examine the Young's modulus, applying the compression mode. Measuring the adhesion force, however, was performed using the tensile mode of the machine. Thus, the test samples needed an additional extension along the sample height, and a  $\sim 4$  cm long PDMS block was attached on the test sample by  $\text{O}_2$  plasma and an epoxy glue, as shown in Fig. 1b. After 2 h for complete fastening, one side of the test sample was attached on the PS dish, and the other side with the extension was held by a holder attached the machine.

For the adhesion test, after fastening the extension, the PDMS surface was treated with (1) no  $\text{O}_2$  plasma (PX) or (2)  $\text{O}_2$  plasma (PO) for 1 min before being attached on the PS dish. Furthermore, the PDMS–PS attachment was preserved with (1) no annealing (AX) or (2) annealing (AO) at 65 °C for 1 h in an oven. Thus, the experimental groups were set as PXAX, PXAO, POAX, and POAO. In addition, the PDMS–PS adhesion was measured with and without treating PS surfaces with  $\text{O}_2$  plasma. Five test samples were examined for each condition.

## 2.4 Cell culture

Two types of myoblasts, C2C12 cells and skeletal muscle progenitor (SMP) cells, were used. The standard protocol from ATCC was used to culture C2C12s in a growth medium (GM) consisting of high-glucose Dulbecco's modified Eagle's medium (DMEM; ThermoFisher Scientific) supplemented with 10% fetal bovine serum (FBS; ThermoFisher Scientific) and 1% penicillin–streptomycin (P/S; ThermoFisher Scientific). SMPs were cultured in GM consisting of an 1:1 mixture of DMEM and Ham's F-10 nutrient mixture (ThermoFisher Scientific), 20% FBS, 1% P/S, and 2.5 ng/ml basic fibroblast growth factor (bFGF; ThermoFisher Scientific) (Ruas et al. 2012). C2C12s and SMPs were kept at less than 70% and 50% confluency, respectively, in an incubator at 37 °C and 5% CO<sub>2</sub>, and the GM was changed every 72 h. The culture dishes were pre-coated with a collagen solution overnight and dried before being used for cell culture.

## 2.5 Cell growth and differentiation on APTES

We investigated the effects of APTES on the proliferation and differentiation (fusion) of C2C12s and SMPs. PS culture dishes were coated with the collagen solution, and APTES was coated or not on top of the collagen.

Myoblasts were trypsinized, collected, and seeded on PS dishes coated with collagen and APTES, and specific GMs were provided for each type of myoblast for 1 day to allow the cells to adhere and settle down at 37 °C and 5% CO<sub>2</sub>. From the next day (D1), we exchanged GM with differentiation medium (DM) consisting of high-glucose DMEM, 5% horse serum (HS; ThermoFisher Scientific), and 1% penicillin–streptomycin. DM was changed every other day, and the PS dishes were kept in the incubator at 37 °C and 5% CO<sub>2</sub> for 6 days (D1–D6) for C2C12 and for 4 days (D1–D4) for SMP.

## 2.6 Immunostaining and imaging

We fixed the cells using 10% formalin for 20 min at room temperature and permeabilized with 0.1% Triton x-100 for 10 min at room temperature. Then, the nuclei and the cytoskeleton were labelled with DAPI (ThermoFisher Scientific) and Alexa Fluor 488 Phalloidin (ThermoFisher Scientific), respectively, for 40 min at room temperature. The stained cells were imaged using a ZEISS inverted fluorescence microscope (Cell observer).

## 3 Results and discussion

### 3.1 The mixing ratio ( $R$ , base/curing agent) determines the mechanical properties of PDMS

We investigated roof collapse (sagging) in PDMS microchannels with  $R$  of 10, 20, 30 and 40 to examine the range of mixing ratios suitable for fabricating microfluidic devices. Microchannels made of PDMS often present design challenges, especially sagging of low aspect ratio channels (ratio between the height ( $H$ ) and the width ( $W$ ),  $H/W$ ). With the PDMS mixing ratio that is generally used ( $R=10$ ), structures with low aspect ratios ( $H/W \leq 0.05$ ) may show sagging during fabrication due to the adhesion (or van der Waals attraction) between PDMS and the substrate, not the effect of gravity (Huang et al. 2005; Melin and Quake 2007; Qin et al. 2010; Zhou et al. 2005). Here we used microchannels with an aspect ratio of 0.06, to meet the design principle of avoiding sagging.

After curing the PDMS microfluidic devices, we cleaned and gently attached the devices on glass slides with and without any additional moderate tapping, which is usually applied to secure the adhesion of PDMS to a substrate (Fig. 2). Opaque areas indicate lack of attachment of PDMS on the glass. Without tapping, the microchannels did not sag irrespective of  $R$ , even though PDMS devices with  $R=30$  and 40 were very soft and sticky, which made the handling of the device difficult. When a mild load (gentle tapping) was applied, sagging was observed. However, for lower  $R$  (10 and 20), sagging was eliminated by elastic strain recovery, reconnecting the channel. Immediate recovery was observed with  $R=10$ , but it took  $\sim 20$  s to recover from sagging with  $R=20$ . With higher  $R$  (30 and 40), sagging became permanent, which indicated that the adhesion to the substrate was greater than the energy for the

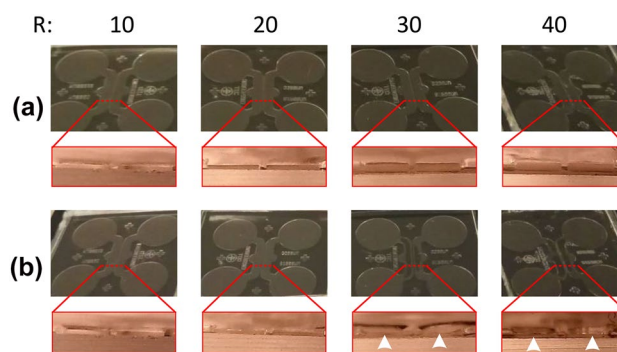


**Fig. 2** Attachment of PDMS microfluidic devices **a** without moderate tapping and **b** after moderate tapping. Top view and cross section images of the microchannels.  $R$  is shown above the images for each PDMS device. Moderate tapping caused the sagging of the microchannels with  $R=30$  and 40, as shown in the cross section image. The white arrows indicate sagging in the device

elastic strain recovery. We concluded that  $R > 20$  should not be considered for microfluidic devices, and the remainder of the experiments were performed with PDMS with  $R \leq 20$  (leakage test included  $R > 20$  to visualize the feasibility of higher  $R$  for microfluidic devices).

We further measured the Young’s modulus of the PDMS by applying compression to cylindrical test samples with various  $R$  (Fig. 3). Young’s modulus,  $E$ , is defined as

$$E = \frac{\Delta\sigma}{\Delta\varepsilon}, \tag{1}$$

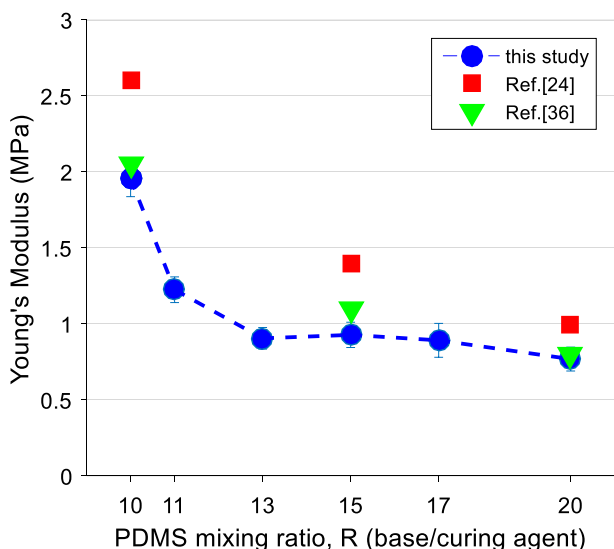


**Fig. 3** Measured Young’s modulus of PDMS with respect to the mixing ratio,  $R$ . The error bar represents the standard deviation of the data. The result is compared with other studies

where  $\Delta\sigma$  is the change of the stress per surface area, and  $\Delta\varepsilon$  is the corresponding change in height of a sample. As expected, the stiffness of PDMS decreased as  $R$  increased. However, the measured ratios suggest a non-linear relationship between the stiffness and PDMS mixing ratio, as shown in Fig. 3, including a comparison with other studies (Wang et al. 2014; Young and Lovell 2011).

We measured the contact angle (CA) and calculated the surface free energy (SFE) of the PDMS, using cylindrical test samples with various  $R$ . Higher SFE yields lower CA, and higher adhesion. The adhesion (the work of adhesion,  $W$ ) of PDMS on a substrate can be defined in terms of energy by Young–Dupre equation (Dupré and Dupré 1869; Huang et al. 2005; Schrader 1995) as

$$W = \gamma_{\text{PDMS/air}} + \gamma_{\text{substrate/air}} - \gamma_{\text{PDMS/substrate}}, \tag{2}$$

where  $\gamma_{\text{PDMS/air}}$ ,  $\gamma_{\text{substrate/air}}$ , and  $\gamma_{\text{PDMS/substrate}}$  are the SFEs of PDMS and the substrate and the interfacial energy, respectively. It should be noted that increasing the SFEs of the PDMS and the substrate increases the adhesion, whereas increasing interfacial energy decreases adhesion. In this work, we aimed to enhance the SFEs of PDMS and PS for increased PDMS–PS bonding, assuming minimal variation of the interfacial energy of PDMS/PS with respect to PDMS mixing ratio.

The measured CAs and SFEs of PDMS are illustrated in Fig. 4. The cylindrical PDMS test samples used for the CA measurements were grouped in two conditions: (1) without  $\text{O}_2$  plasma or annealing (PXAX) and (2) with both  $\text{O}_2$  plasma and annealing (POAO). After the treatment, the test samples were quarantined for 1 h, being kept away from the dust. Other conditions, such as PXAO and POAX, were not considered, because those conditions were not practical to modify the PDMS surfaces, specifically annealing without

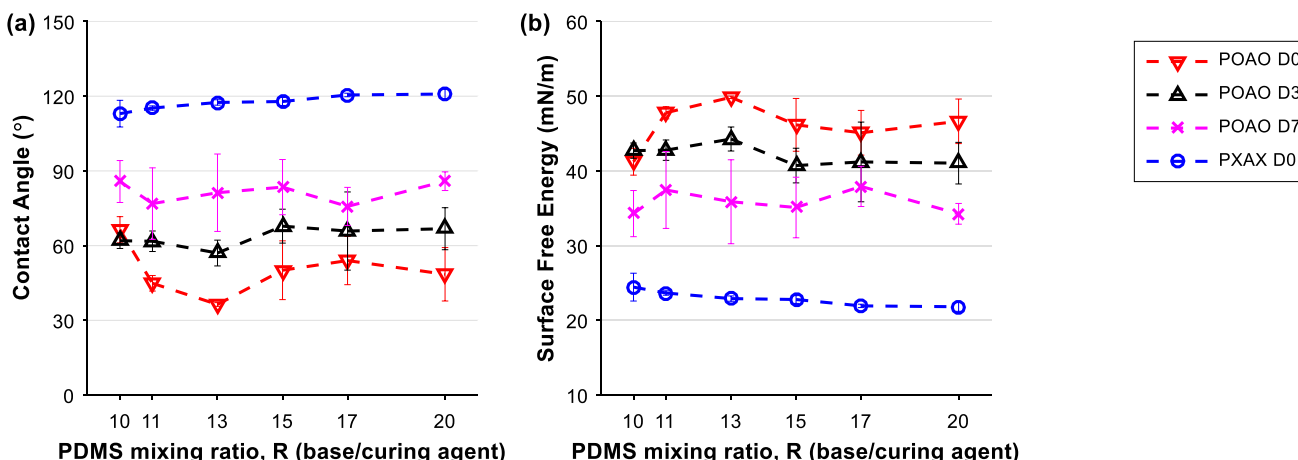


**Fig. 4 a** Contact angle measurements of PDMS with respect to  $R$ . **b** SFEs calculated using the CA measurements in **a**. PXAX indicates surfaces without  $\text{O}_2$  plasma or annealing, and POAO surfaces were

treated with both  $\text{O}_2$  plasma and annealing. D0, D3 and D7 indicate the number of days after the surface was treated. The error bars represent the standard deviation of the data

O<sub>2</sub> plasma (no SFE change) and 1-h room temperature incubation after O<sub>2</sub> plasma (recovery of hydrophobicity). The properties were measured on the day of the surface treatment (D0) as well as 3 days (D3) and 7 days (D7) after treatment. As expected, the PXAX condition resulted in the highest CAs and the lowest SFEs of PDMS surfaces, indicative of hydrophobic surfaces (CA > 90°), and showed similar CA values for all *R*. Importantly, the observed hydrophilicity (CA < 90°) of the POAO surfaces, was kept for a week, although the hydrophilicity gradually decreased. These data suggests that annealing induces more stable surface presentation of silanol (Si–OH) groups formed by O<sub>2</sub> plasma, slowing the recovery process of the surface from hydrophilic to hydrophobic.

We observed that for the surface presenting the highest hydrophilicity, *R* = 13, the treated PDMS surface exhibited a CA of ~35° and an SFE of ~50 mN/m, while the untreated PDMS surface showed ~110° CA and ~23 mN/m SFE. The CA measurements on samples with higher *R<sub>s</sub>* (*R* > 13) exhibited larger standard deviations at D0, indicating rather unstable states of the surfaces. In addition, the results on D7 show large standard deviations for all *R<sub>s</sub>*, suggesting that the recovering hydrophobicity leads to variability in the states of the surfaces.

### 3.2 PDMS–PS bonding

The adhesion of PDMS and PS surfaces was investigated using cylindrical PDMS test samples (8 mm in diameter glued to an extension block). Using the tensile mode, the testing machine pulled the extension block until the sample detached, and the force applied was determined. First, we measured PDMS–PS bonding without treating the PS surface with O<sub>2</sub> plasma. The PDMS samples were treated with O<sub>2</sub> plasma (PO) or left untreated (PX) and were attached

onto the PS dish. Next, we either annealed the samples at 65°C for an hour (AO) or left them at room temperature (AX). Therefore, the four conditions tested for PDMS–PS bonding were POAO, POAX, PXAO, and PXAX (Fig. 5a). On the PS surface that was not treated with O<sub>2</sub> plasma, PDMS in PXAX condition showed the lowest adhesion. The adhesion of PDMS in PXAO condition was slightly increased, while PDMS in POAX and POAO conditions exhibited the highest adhesion. However, all the conditions without O<sub>2</sub> plasma treatment of the PS surface showed comparable adhesion forces.

Next, we treated the PS surface with O<sub>2</sub> plasma. The CA and SFE of the PS dishes in the different conditions is presented in Table 1. It should be noted that the annealing of the PS surface was followed after the attachment of PDMS to the PS dishes. The PDMS samples were prepared as described above: POAO, POAX, PXAO, and PXAX (Fig. 5b). The adhesion of PDMS to the treated PS surface was consistently higher in the POAO condition than in the POAX condition, which did not undergo annealing. In fact, the condition with the highest adhesion, the POAO condition attached to the plasma-treated PS, showed about 6 times higher adhesion than the attachment of PDMS (PXAX) to the untreated PS surface. Interestingly, the unannealed PDMS (POAX) did not

**Table 1** Properties of PS dish surface with and without O<sub>2</sub> plasma and annealing

	PXAX	POAO D0	POAO D3	POAO D7
CA (°)	75 ± 2.8	30 ± 5.6	35 ± 1.5	35 ± 2.0
SFE (mN/m)	38 ± 1.0	51 ± 1.0	50 ± 0.3	50 ± 0.4

PX no O<sub>2</sub> plasma, PO O<sub>2</sub> plasma, AX no annealing, AO annealing, *D*-number days after the treatment

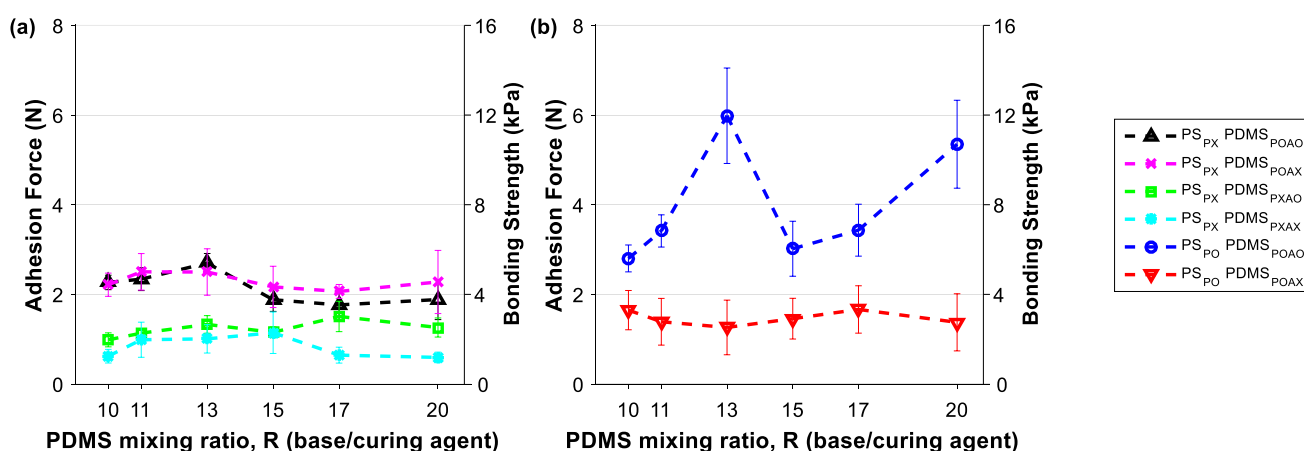


**Fig. 5** Adhesion of cylindrical PDMS test samples on PS surfaces. PDMS–PS bonding on **a** non-treated PS surface and **b** O<sub>2</sub> plasma-treated PS surface. The adhesion force values are also represented in pressure as the bonding strength

show efficient adhesion, even on the treated PS surface. It is noted that  $\gamma_{\text{substrate/air}} \gg \gamma_{\text{substrate/liquid}}$ , implying that potentially  $\gamma_{\text{PDMS/air}} \gg \gamma_{\text{PDMS/liquid}}$ ; thus, the adhesion of PDMS on a wet surface would become weaker (Huang et al. 2005; Johnson et al. 1971). As the annealing process heated the interface of the PDMS–PS bonding, it could be inferred that the PDMS surface was conceivably further dehydrated, yielding stronger adhesion. It is noted that typical bonding strength of PDMS and glass after applying  $\text{O}_2$  plasma to PDMS is  $\sim 0.4$  MPa (Gajasinghe et al. 2014) which is, indeed, much higher than the bonding strength of PDMS–PS, even with the surface treatments and annealing step that we introduce here.

We further investigated the significance of the measured adhesion force for leakage in microfluidic devices. We used devices consisting of two parallel microchannels. After cleaning the devices, they were treated with  $\text{O}_2$  plasma for 1 min and attached onto the plasma-treated PS dishes. The dishes with the devices were then annealed in an oven at  $65^\circ\text{C}$  for 1 h. Next, we filled the microchannels with water colored (red or green) for improved visualization and kept the devices in an oven at  $37^\circ\text{C}$  overnight. Due to the long-lasting hydrophilicity, the channels were easily filled with water by capillarity on the following day. 24 h later, we observed that the water was kept in the channels without leakage in all conditions, except for the case of  $R=10$  (Fig. 6). From this test, it can be inferred that bonding strength higher than  $\sim 5$  kPa yields efficient PDMS–PS bonding.

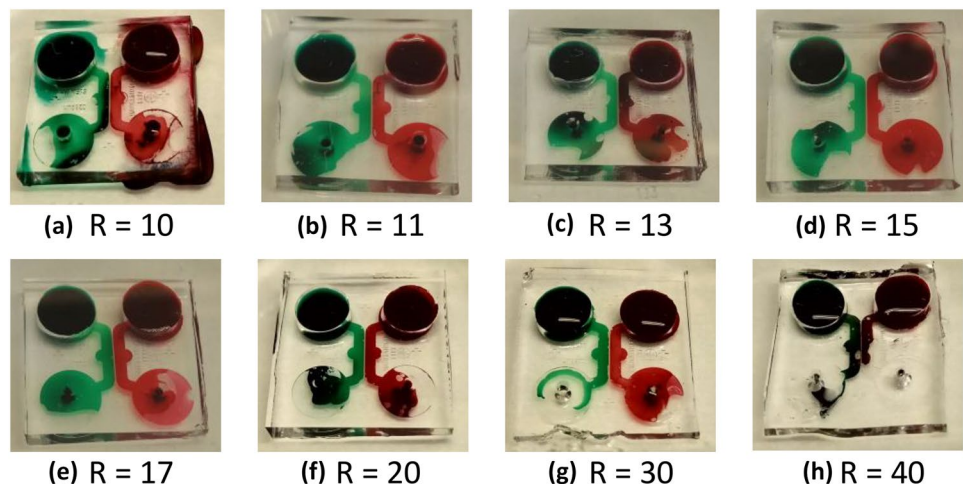
We also tested the leakage in PDMS devices with  $R=30$  and 40, and both ratios showed good sealing properties. However, the low stiffness of these devices presented challenges during handling. In particular, in the device with  $R=40$  some structures were disrupted during the peeling process, and we observed crossover of the colored waters between channels, even though the adhesion was good. In addition, the channels sagged during the attachment.

### 3.3 Cell culture on APTES and PDMS–PS microfluidic cell-culture system

We investigated the effects of APTES on myotube maturation, using C2C12s and primary SMPs. As described in the Sect. 2, C2C12s or SMPs were cultured either on collagen ECM or on APTES coated collagen ECM. On D6 for C2C12 and D4 for SMP, the cells were fixed and imaged (Fig. 7a). We observed the size of the myotubes and the number of nuclei in a myotube to assess the maturity of myotubes. The C2C12 cells presented similar sizes of myotubes and number of nuclei in a myotube in the collagen surfaces with or without APTES. In contrast, few primary SMPs survived on APTES coated collagen ECM. We concluded that APTES could be used with immortalized cells such as C2C12. However, for stem cell-like and primary cells, which are very sensitive to their microenvironment, APTES should be avoided.

Next, we cultured SMPs in the PDMS–PS microfluidic devices which were fabricated with  $R=11$  and  $\text{O}_2$  surface plasma treatment of PDMS and PS as well as annealing, i.e.,  $\text{PS}_{\text{PO}} \text{PDMS}_{\text{POAO}}$ . Before loading SMPs in the device, the device was exposed to UV light in a laminar flow cell-culture hood for 20 min for sterilization. Then, the device was filled with the collagen solution overnight. After aspirating the collagen solution, we added  $100 \mu\text{l}$  growth medium (GM) in each reservoir and kept the device in an incubator at  $37^\circ\text{C}$  until the flow was stabilized in the device. In the meantime, SMPs were trypsinized and prepared in Eppendorf tubes. The prepared SMPs were suspended in  $3.5 \mu\text{l}$  GM and carefully introduced to the device through the inlet port. The hydrostatic pressure formed by the cell suspension allowed the cells to spread through the device. We kept the device in an incubator at  $37^\circ\text{C}$  and 5%  $\text{CO}_2$  overnight with GM. Then, we changed the medium to differentiation medium (DM), which was replaced daily for the next 4 days, to form myotubes. A fluorescent image of myotubes formed

**Fig. 6** Optical images of leakage on PDMS–PS devices with various PDMS  $R_s$ . Samples were imaged after 24 h, when additional colored water was added for improved visualization of leakage



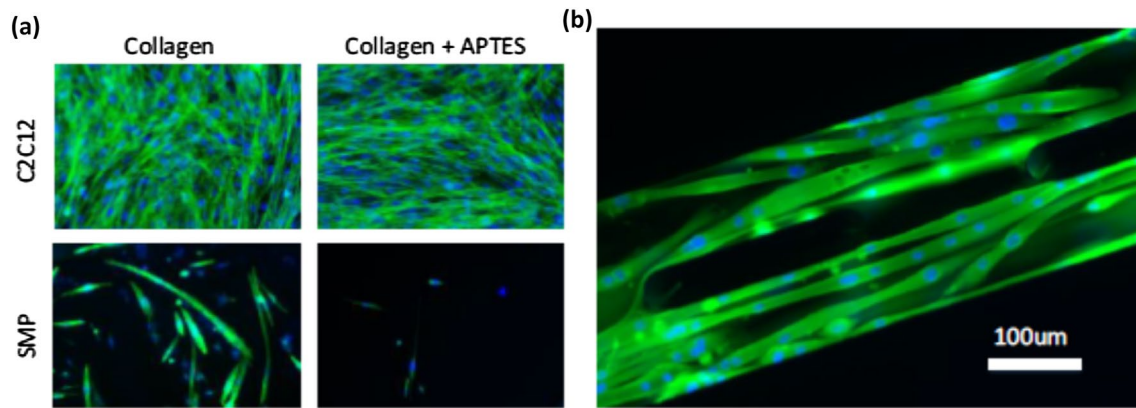


**Fig. 7** Fluorescent images of myotubes derived from: **a** C2C12s or SMPs cultured in PS dishes, and **b** SMPs cultured in a PDMS–PS microfluidic cell-culture system. Nuclei are in blue (DAPI), and the myotubes are shown in green (Alexa Fluor 488 Phalloidin). (Color figure online)

in the microfluidic device is shown in Fig. 7b. SMPs formed long, multinucleated myotubes in the devices, indicating that the devices are appropriate for myotube maturation.

## 4 Conclusion

We have achieved a reversible and leakage-free bonding of PDMS to PS without use of potentially toxic chemical agents (e.g., APTES). This system paves the way to construct PDMS–PS microfluidic cell-culture systems with reversible bonding. In our approach, PDMS–PS bonding was enhanced by tuning the surface free energy of PDMS and PS surfaces; specifically, the surface free energy of PDMS was tuned by the mixing ratio (base versus curing agent) and  $O_2$  plasma surface treatment. Furthermore, this high-surface free energy lasted for more than 72 h with an additional annealing process (note that the surface free energy decreased within minutes without annealing). With our approach, we achieved a bonding strength for PDMS–PS of approximately 12 kPa ( $\sim 6$  N). We further concluded that  $\sim 5$  kPa bonding strength was enough to achieve reversible and leakage-free PDMS–PS bonding. We also tested our PDMS–PS microfluidic cell-culture system by culturing primary SMPs and differentiating them into myotubes. We observed the formation of long myotubes containing a large number of nuclei, indicating the formation of healthy and the mature myotubes. We propose that the reversible and leakage-free PDMS–PS system that we introduce here will advance the culture and analysis of primary cells in microfluidics systems.

**Acknowledgements** This work was supported by grants from the Human Frontier Science Program Young Investigator Award (AIT, RGY0082-2014), the Swedish Research Council (AIT; 2015-03520), NSERC Discovery Grant of Canada.

## Compliance with ethical standards

**Conflict of interest** The authors declare that they have no conflict of interest.

## References

- Abdelgawad M, Watson MWL, Young EWK, Mudrik JM, Ungrin MD, Wheeler AR (2008) Soft lithography: masters on demand. *Lab Chip* 8:1379–1385
- Duffy DC, McDonald JC, Schueller OJA, Whitesides GM (1998) Rapid prototyping of microfluidic systems in poly(dimethylsiloxane). *Anal Chem* 70:4974–4984
- Dupré A, Dupré P (1869) *Théorie mécanique de la chaleur*. Gauthier-Villars, Paris
- Friend J, Yeo L (2010) Fabrication of microfluidic devices using polydimethylsiloxane. *Biomicrofluidics* 4:026502
- Gajasinghe RWRL et al (2014) Experimental study of PDMS bonding to various substrates for monolithic microfluidic applications. *J Micromech Microeng* 24:075010
- Halldrsson S, Lucumi E, Gómez-Sjöberg R, Fleming RMT (2015) Advantages and challenges of microfluidic cell culture in polydimethylsiloxane devices. *Biosens Bioelectron* 63:218–231
- Haubert K, Drier T, Beebe D (2006) PDMS bonding by means of a portable, low-cost corona system. *Lab Chip* 6:1548–1549
- Huang YY, Zhou W, Hsia KJ, Menard E, Park J-U, Rogers JA, Alleyne AG (2005) Stamp collapse in soft lithography. *Langmuir* 21:8058–8068
- Igata E, Arundell M, Morgan H, Cooper JM (2002) Interconnected reversible lab-on-a-chip technology. *Lab Chip* 2:65–69
- Im SG, Bong KW, Lee C-H, Doyle PS, Gleason KK (2009) A conformal nano-adhesive via initiated chemical vapor deposition for microfluidic devices. *Lab Chip* 9:411–416
- Johnson KL, Kendall K, Roberts AD (1971) Surface energy and the contact of elastic solids. *Proc R Soc Lond A Math Phys Sci* 324:301–313
- Johnston ID, McCluskey DK, Tan CKL, Tracey MC (2014) Mechanical characterization of bulk Sylgard 184 for microfluidics and microengineering. *J Micromech Microeng* 24:035017
- Kovarik ML, Gach PC, Orloff DM, Wang Y, Balowski J, Farrag L, Allbritton NL (2012) Micro total analysis systems for cell biology and biochemical assays. *Anal Chem* 84:516–540



- Kovarik ML et al (2013) Micro total analysis systems: fundamental advances and applications in the laboratory, clinic, and field. *Anal Chem* 85:451–472
- Lamberti A, Quaglio M, Sacco A, Cocuzza M, Pirri CF (2012) Surface energy tailoring of glass by contact printed PDMS. *Appl Surf Sci* 258:9427–9431
- Le Berre M, Crozatier C, Velve Casquillas G, Chen Y (2006) Reversible assembling of microfluidic devices by aspiration. *Microelectron Eng* 83:1284–1287
- Lee NY, Chung BH (2009) Novel poly(dimethylsiloxane) bonding strategy via room temperature “Chemical Gluing”. *Langmuir* 25:3861–3866
- Lee JN, Park C, Whitesides GM (2003) Solvent compatibility of poly(dimethylsiloxane)-based microfluidic devices. *Anal Chem* 75:6544–6554
- Li Z, Yang J, Li K, Zhu L, Tang W (2017) Fabrication of PDMS microfluidic devices with 3D wax jetting. *RSC Adv* 7:3313–3320
- Liu M, Sun J, Chen Q (2009) Influences of heating temperature on mechanical properties of polydimethylsiloxane. *Sens Actuators A Phys* 151:42–45
- Lowe AM, Ozer BH, Wiepz GJ, Bertics PJ, Abbott NL (2008) Engineering of PDMS surfaces for use in microsystems for capture and isolation of complex and biomedically important proteins: epidermal growth factor receptor as a model system. *Lab Chip* 8:1357–1364
- Melin J, Quake SR (2007) Microfluidic large-scale integration: the evolution of design rules for biological automation. *Annu Rev Biophys Biomol Struct* 36:213–231
- Ochsner M, Dusseiller MR, Grandin HM, Luna-Morris S, Textor M, Vogel V, Smith ML (2007) Micro-well arrays for 3D shape control and high resolution analysis of single cells. *Lab Chip* 7:1074–1077
- Palchesko RN, Zhang L, Sun Y, Feinberg AW (2012) Development of polydimethylsiloxane substrates with tunable elastic modulus to study cell mechanobiology in muscle and nerve. *PLoS One* 7:e51499
- Qin D, Xia Y, Whitesides GM (2010) Soft lithography for micro- and nanoscale patterning. *Nat Protoc* 5:491–502
- Ruas JL et al (2012) A PGC-1 $\alpha$  isoform induced by resistance training regulates skeletal muscle hypertrophy. *Cell* 151:1319–1331
- Ryan JA (2008) Evolution of cell culture surfaces. *BioFiles* 3(8):21
- Schrader ME (1995) Young-dupre revisited. *Langmuir* 11:3585–3589
- Seghir R, Arscott S (2015) Extended PDMS stiffness range for flexible systems. *Sens Actuators A Phys* 230:33–39
- Shiroma LS, Piazzetta MHO, Duarte-Junior GF, Coltro WKT, Carrilho E, Gobbi AL, Lima RS (2016) Self-regenerating and hybrid irreversible/reversible PDMS microfluidic devices. *Sci Rep* 6:26032
- Sonney S, Shek N, Moran-Mirabal JM (2015) Rapid bench-top fabrication of poly(dimethylsiloxane)/polystyrene microfluidic devices incorporating high-surface-area sensing electrodes. *Biomicrofluidics* 9:026501
- Sunkara V, Park D-K, Hwang H, Chantiwas R, Soper SA, Cho Y-K (2011) Simple room temperature bonding of thermoplastics and poly(dimethylsiloxane). *Lab Chip* 11:962–965
- Tanaka N, Ota H, Fukumori K, Miyake J, Yamato M, Okano T (2014) Micro-patterned cell-sheets fabricated with stamping-force-controlled micro-contact printing. *Biomaterials* 35:9802–9810
- Tang L, Lee NY (2010) A facile route for irreversible bonding of plastic-PDMS hybrid microdevices at room temperature. *Lab Chip* 10:1274–1280
- Teixeira AI, Ilkhanizadeh S, Wigenius JA, Duckworth JK, Inganäs O, Hermanson O (2009) The promotion of neuronal maturation on soft substrates. *Biomaterials* 30:4567–4572
- Vézy C, Haddour N, Dempsey NM, Dumas-Bouchiat F, Frénéa-Robin M (2011) Simple method for reversible bonding of a polydimethylsiloxane microchannel to a variety of substrates. *Micro Nano Lett* 6:871–873
- Wang L, Acosta MA, Leach JB, Carrier RL (2013) Spatially monitoring oxygen level in 3D microfabricated cell culture systems using optical oxygen sensing beads. *Lab Chip* 13:1586–1592
- Wang Z, Volinsky AA, Gallant ND (2014) Crosslinking effect on polydimethylsiloxane elastic modulus measured by custom-built compression instrument. *J Appl Polym Sci* 131:41050
- Wasay A, Sameoto D (2015) Gecko gaskets for self-sealing and high-strength reversible bonding of microfluidics. *Lab Chip* 15:2749–2753
- Wheeler AR, Trapp G, Trapp O, Zare RN (2004) Electroosmotic flow in a poly(dimethylsiloxane) channel does not depend on percent curing agent. *Electrophoresis* 25:1120–1124
- Xia Y, Whitesides GM (1998) Soft Lithography. *Annu Rev Mater Sci* 28:153–184
- Xie S, Wu J, Tang B, Zhou G, Jin M, Shui L (2017) Large-area and high-throughput PDMS microfluidic chip fabrication assisted by vacuum airbag laminator. *Micromachines* 8:218
- Young RJ, Lovell PA (2011) Introduction to polymers, 3rd edn. CRC Press, Boca Raton
- Zhou W, Huang Y, Menard E, Aluru NR, Rogers JA, Alleyne AG (2005) Mechanism for stamp collapse in soft lithography. *Appl Phys Lett* 87:251925

**Publisher's Note** Springer Nature remains neutral with regard to jurisdictional claims in published maps and institutional affiliations.